

New phases of  $sp^2$ -bonded boron nitride: the 12R and 24R polytypes

F. F. Xu,\* Y. Bando and M. Hasegawa

National Institute for Materials Science, Tsukuba, Ibaraki 305, Japan. E-mail: xu.fangfang@nims.go.jp

Received (in Cambridge, UK) 4th April 2002, Accepted 30th May 2002

First published as an Advance Article on the web 11th June 2002

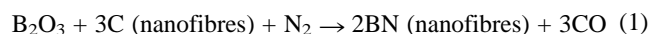
$sp^2$ -Bonded polytypes of graphite-like boron nitride are evidenced in the approximately twin-related bicrystal-like BN nanofibres synthesized by a high-temperature substitution reaction between carbon nanofibres and boron oxides in  $N_2$  atmosphere; the material shows a main 12R phase of A'ABC/C' CAB/B'BCA packing and a minor 24R phase with an A'ABC/BB'C'A'/C' CAB/... packing sequence.

Boron nitride has two structural modifications: graphite-like BN ( $g$ -BN) with hexagonal ( $h$ -BN) and rhombohedral ( $r$ -BN) structures,<sup>1,2</sup> and the diamond-like BN with wurtzite and zincblende structures.<sup>3,4</sup> In the past decade, graphite-like BN has been receiving attention since BN nanotubes are developed by curling the BN sheets to form a tube-shape.<sup>5,6</sup> Boron nitride, either in the form of nanotubes or thin films, exhibits numerous interesting physical properties<sup>7,8</sup> and promising future applications as, for example, field-emitting devices<sup>9,10</sup> and hydrogen storage materials.<sup>11–13</sup> Ma *et al.*<sup>13</sup> have recently succeeded in storing as high as 3wt% of hydrogen in BN nanotubes. It has been documented that defect structures in  $g$ -BN would provide suitable trapping sites for hydrogen storage.<sup>12</sup> The present polytypic structures highlight the exploration of  $g$ -BN for this kind of usage.

Layered  $g$ -BN with covalent bonds of trigonal coordination, *i.e.*,  $sp^2$ , displays a rigid flat network of  $B_3N_3$  hexagons on the layer plane while stacking of layers involves different patterns. The two most stable structural modifications are  $h$ -BN and  $r$ -BN, which consist of alternating layers of AA'AA' and ABCABC sequences, respectively. Some metastable BN phases also have been reported and include ABAB, AAAA and ADAD structures.<sup>14,15</sup> The co-existence of different packing structures has led to the formation of faults in  $g$ -BN. However, long-range ordering of intergrowths, *i.e.*, polytypism has never been observed in  $sp^2$ -bonded materials such as graphite and  $g$ -BN. It has widely been documented that materials with  $sp^3$  bonds of tetrahedral coordination may show polytypism as is well known in SiC, AlN and ZnS, due to the variations in the stacking of

close-packed layers. The  $sp^3$ -bonded nitrides of the group 13 elements in the periodic table, *e.g.* BN, AlN and GaN, show a variety of polytypic structures. The 5H-BN phase<sup>16</sup> and 9R-GaN phase<sup>17</sup> have been reported recently. In this communication, we report the polytypism of  $sp^2$ -bonded graphite-like BN as discovered in the approximately twin-related  $g$ -BN nanofibres synthesized by substitution reaction at 1700 °C.

The well-aligned carbon nanofibres were prepared using a CVD method described before.<sup>18</sup> A Ti substrate was used on which Co nano-particles were dispersed. The BN nanofibres were then synthesized employing a designed substitution reaction,<sup>19</sup> as expressed by eqn. (1):



Transmission electron microscopy (TEM) observation of the present material shows numerous ( $\sim 10$  wt%) bicrystal-like fibres as typically shown in Fig. 1(a). The electron energy-loss spectrum (EELS) (see Fig. 1(b)) indicates a BN phase with graphite-like structure by noting the appearance of the boron peak characteristic of  $\pi$ -bonds. A trace amount of C is detected, which is always present when using the present substitution synthesis from C nanofibres. TEM observation from various directions by tilting the specimen reveals the general morphology of these BN nanofibres as schematically shown in Fig. 1(c). The two variants are twin-related with the twin plane on  $\{01\bar{1}1\}$  of the  $h$ -BN. The thickness, *i.e.*, the dimension approximately along the view direction of Fig. 1(a) is  $\sim 90$  nm. It is noted from Fig. 1(a) that each variant of the twin-related bicrystal shows dense fault contrast, indicative of various displacements parallel to the BN layers upon packing. Long-range ordering has been observed in these faulted nanofibres.

Fig. 2 shows the  $a$ -projected diffraction pattern of the polytypic phase obtained from an individual  $g$ -BN fibre. A four-fold superlattice along the  $c$ -axis is evident, an indication of a stacking period consisting of four BN layers. The diffraction pattern corresponds to a pseudo-rhombohedral structure. The stacking sequence of the polytypic structure has been deter-

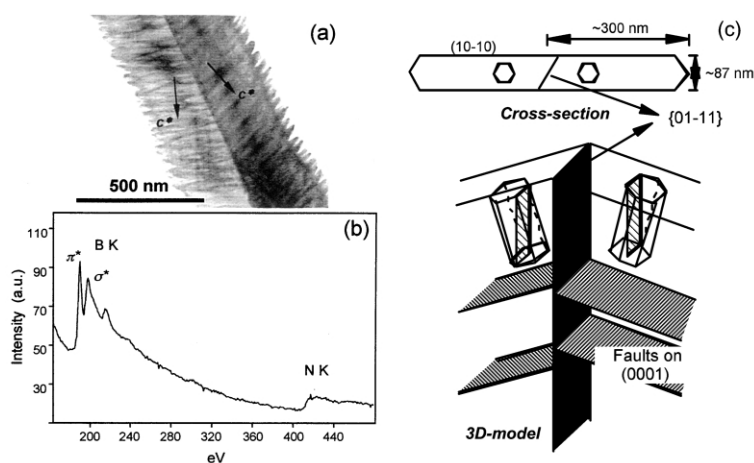
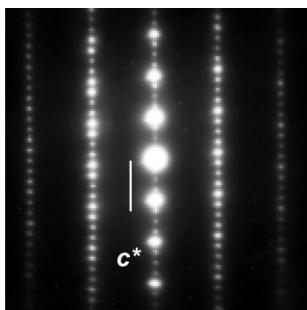
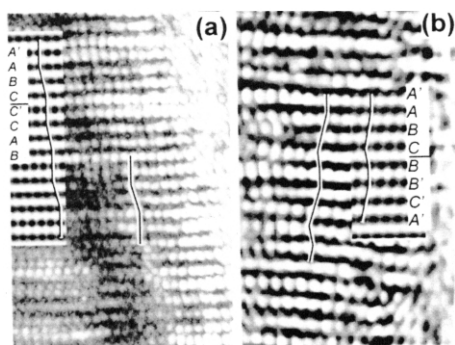


Fig. 1 (a) An individual twin-related bicrystal-like fiber of graphite-like BN with its EELS spectrum (b) and schematic model (c). Dense fault contrast is noted where polytypes are involved.



**Fig. 2** The  $[2-1-10]$ -projected diffraction pattern of the present *g*-BN polytypic phase.

mined by a high-resolution electron microscopy (HREM) study. Two polytypic structures (Fig. 3(a) and (b)) were observed. Both show an identical A'ABC-type stacking sequence in a four-layer subunit. However, the packing patterns of subunits vary in different polytypes. Fig. 3(a) illustrates a twelve-layer packing period, namely the 12R (R represents rhombohedral symmetry) polytype. The complete packing sequence in a super-unit is described as A'ABC/C' CAB/B'BCA. Fig. 3(b) shows a 24R polytype, which consists of twenty-four BN layers and the structure is described as A'ABC/BB'C'A'/C' CAB/AA'B'C'/B'BCA/CC'A'B'. Each four-layer subunit, *e.g.* the A'ABC sequence is the intergrowth of one *h*-BN unit cell (A'A) and one *r*-BN unit cell (ABC), which share the common A layer. In the 12R structure, the packing of two neighboring subunits employs an *h*-BN packing pattern across the boundary, *e.g.* C/C'. However in the 24R structure, the two neighboring subunits exhibit a twin-related stacking mode in the vicinity of the boundary, *e.g.* BC/B near the boundary between the first and second subunit. When the two BN layers at either side of the subunit boundary have different B<sub>3</sub>N<sub>3</sub> hexagon graphene structures, *i.e.* different type of labels (letters with and without dash), the *h*-BN-type stacking (AA'-stacking) is employed, which is the only packing pattern that is considered to be stable. Then, the 12R polytype is formed. However, when the two BN layers near the boundaries have the same graphene structure, AB-stacking is apparently energetically more favourable than AA'-stacking. Then, the 24R polytype is generated. It seems that a twin related stacking in the vicinity of the subunit boundary is more favourable than the *r*-BN type stacking, *i.e.* for example, BC/B rather than BC/A packing across the boundary. The simulated images calculated based on both the 12R and 24R



**Fig. 3** HREM images of the 12R (a) and the 24R (b) polytypes. The simulated images of different polytypes are also shown.

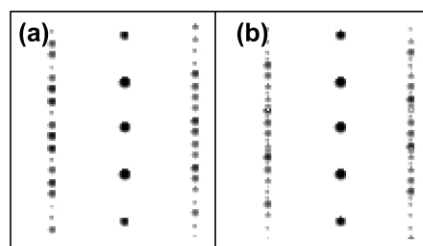


**Fig. 4** The calculated dynamic electron diffraction patterns of (a) the 12R and (b) the 24R polytypes.

packing sequences are shown in Fig. 3(a) and (b), respectively, while the calculated diffraction patterns are illustrated in Fig. 4(a) and (b). It is noted that the calculated images and diffraction patterns match well with the experimental observations.

The *h*-BN and *r*-BN are the stable phases at low temperatures.<sup>15</sup> The extreme high synthesis temperature ( $\sim 1700$  °C) could have been responsible for the stabilization of the polytypic structures of graphite-like BN. Whether or not the marginal C impurities have played a role in the formation of polytypes is still unknown. Nevertheless, the present discovery suggests a practical possibility for the formation of various polytypic structures based on  $sp^2$ -bonded graphite-like BN. Since the polytypic phases usually exhibit different physicochemical properties from the parent phase,<sup>20</sup> the development of different polytypic phases of *g*-BN opens up broad prospects for modern physical chemistry and materials science.

## Notes and references

- 1 R. S. Pease, *Acta Crystallogr.*, 1952, **5**, 356.
- 2 R. Sato, *J. Phys. Soc. Jpn.*, 1966, **21**, 1623.
- 3 R. H. Wentorf, *J. Chem. Phys.*, 1951, **26**, 956.
- 4 F. P. Bundy and R. H. Wentorf, *J. Chem. Phys.*, 1963, **38**, 1144.
- 5 A. Loiseau, F. Willaime, N. Demoncey, G. Hug and H. Pascard, *Phys. Rev. Lett.*, 1996, **76**, 4737.
- 6 D. Golberg, Y. Bando, M. Eremets, K. Takemura, K. Kurashima and H. Yusa, *Appl. Phys. Lett.*, 1996, **69**, 2045.
- 7 X. Blase, A. De Vita, J. C. Charlier and R. Car, *Europhys. Lett.*, 1994, **28**, 335.
- 8 P. Kral, E. J. Mele and D. Tomanek, *Phys. Rev. Lett.*, 2000, **85**, 1512.
- 9 T. Sugino, K. Tanioka, S. Kawasaki and J. Shirafuji, *Jpn. J. Appl. Phys. II*, 1997, **36**, L463.
- 10 T. Sugino and S. Tagawa, *Appl. Phys. Lett.*, 1999, **74**, 889.
- 11 P. M. Ajayan and T. W. Ebbesen, *Rep. Prog. Phys.*, 1997, **60**, 1025.
- 12 P. Wang, S. Orimo, T. Matsushima, H. Fujii and G. Majer, *Appl. Phys. Lett.*, 2002, **80**, 318.
- 13 R. Ma, Y. Bando, H. Zhu, T. Sato, C. Xu and D. Wu, *J. Am. Chem. Soc.*, 2002, **124**, in press.
- 14 A. Brager, *Acta Physicochim.*, 1939, **11**, 617.
- 15 V. M. Danilenko, A. V. Kurdyumov and A. V. Meike, *Sov. Phys. Crystallogr.*, 1981, **26**, 191.
- 16 S. Komatsu, K. Okada, Y. Shimizu and Y. Moriyoshi, *J. Phys. Chem. B*, 1999, **103**, 3289.
- 17 H. Selke, V. Kirchner, H. Heinke, S. Einfeldt, P. L. Ryder and D. Hommel, *J. Cryst. Growth*, 2000, **208**, 57.
- 18 Y. Bando, K. Ogawa and D. Golberg, *Chem. Phys. Lett.*, 2001, **347**, 349.
- 19 W. Han, Y. Bando, K. Kurashima and T. Sato, *Appl. Phys. Lett.*, 1998, **73**, 3085.
- 20 G. C. Trigunayat, *Solid State Ionics*, 1991, **48**, 3.